**The EMBO Journal** Vol.16 No.16 pp.5098–5112, 1997

# Interaction of DNA-dependent protein kinase with DNA and with Ku: biochemical and atomic-force microscopy studies

**Mariana Yaneva[1], Tomasz Kowalewski[2] and Michael R.Lieber[1,3,4]**

[1]Department of Pathology, Washington University, St Louis, MO 63110, [2]Department of Chemistry, Washington University, St Louis, MO 63130 and [3]Norris Comprehensive Cancer Center, Rm 5425, Mail Stop 73, University of Southern California School of Medicine, 1441 Eastlake Ave, Los Angeles, CA 90033, USA

[4]Corresponding author
e-mail: lieber_m@froggy.hsc.usc.edu

**DNA-dependent protein kinase (DNA-PK or the scid factor) and Ku are critical for DNA end-joining in V(D)J recombination and in general non-homologous double-strand break repair. One model for the function of DNA-PK is that it forms a complex with Ku70/86, and this complex then binds to DNA ends, with Ku serving as the DNA-binding subunit. We find that DNA-PK can itself bind to linear DNA fragments ranging in size from 18 to 841 bp double-stranded (ds) DNA, as indicated by: (i) mobility shifts; (ii) crosslinking between the DNA and DNA-PK; and (iii) atomic-force microscopy. Binding of the 18 bp ds DNA to DNA-PK activates it for phosphorylation of protein targets, and this level of activation is not increased by addition of purified Ku70/86. Ku can stimulate DNA-PK activity beyond this level only when the DNA fragments are long enough for the independent binding to the DNA of both DNA-PK and Ku. Atomic-force microscopy indicates that under such conditions, the DNA-PK binds at the DNA termini, and Ku70/86 assumes a position along the ds DNA that is adjacent to the DNA-PK.**

*Keywords*: atomic-force microscopy/DNA end-joining/DNA-PK/double-strand break repair/Ku70/86

## Introduction

Two proteins that participate in non-homologous double-strand break repair are the heterodimer, Ku70/86 and a 470 kDa kinase activated by DNA termini called DNA-dependent protein kinase (DNA-PK). The repair role of these proteins has been determined genetically based on the fact that mutant mammalian cells are deficient in the repair of radiation- and chemically-induced double-strand breaks and in carrying out physiological processes involving double-strand breaks such as V(D)J recombination (Jackson and Jeggo, 1995; Lieber *et al*., 1997).

In this field, a dominant hypothesis for DNA-PK function is that it exists in a physical complex with the Ku70/86 heterodimer. This heterotrimer model is based on three types of biochemical data. First, immunoprecipitation of Ku out of crude extracts using monoclonal antibodies and human autoimmune sera (that contain anti-Ku antibodies) co-precipitates submolar amounts of DNA-PK (Gottlieb and Jackson, 1993; Suwa *et al*., 1994). Secondly, phosphorylation of the transcription factor Sp1 by DNA-PK depends on the presence of Ku (Gottlieb and Jackson, 1993). Thirdly, a crude extract assay for DNA-PK activity demonstrates a 2- to 8-fold dependence on Ku (Finnie *et al*., 1995). This assay employs DNA–cellulose to pull DNA-associated kinase activity out of the crude extracts.

There are limitations to these approaches in inferring protein complex formation. First, immunoprecipitants, especially at submolar ratios, can be due to non-specific co-precipitation, especially if the complex is only stable over a relatively narrow range of ionic strength. Second, the clearest case where DNA-PK phosphorylation has been shown to be entirely dependent on Ku is for the transcription factor, Sp1 (Gottlieb and Jackson, 1993). However, many other targets can be phosphorylated by DNA-PK in the apparent absence as well as in the presence of Ku. These Ku-independent targets include the p53 peptide (Anderson and Lees-Miller, 1992), the RNA polymerase II CTD tail (Dvir *et al*., 1993), replication protein A (RP-A) (Brush *et al*., 1994; Pan *et al*., 1994), and heat shock protein 90 (hsp90) (Anderson and Lees-Miller, 1992). Third, crude extract assays for DNA-PK activity include many other proteins and contaminating nucleic acids, making it extremely difficult to make clear inferences about a multi-protein complex (Finnie *et al*., 1995). Moreover, apparent null mutants for Ku (xrs5 and 6) still contained a DNA-dependent protein kinase activity detectable even in the low-sensitivity DNA-PK pull-down assay (Singleton *et al*., 1997), again suggesting DNA-PK activity in the absence of Ku.

Because of the uncertainties about the activation of DNA-PK and the nature of the Ku–DNA-PK complex formation, a careful re-evaluation of the biochemical association of Ku and DNA-PK was conducted. We find that both Ku and DNA-PK independently bind to linear DNA, accounting for their association in crude extracts containing DNA fragments. Ku can stimulate DNA-PK if they are each bound to a double-stranded (ds) DNA fragment long enough to permit them to take up adjacent positions. These biochemical studies agree with atomic-force microscopy studies suggesting a model in which Ku binds at DNA ends and moves to internal positions; DNA-PK binds independently to the DNA termini. Once each is on DNA, Ku may activate DNA-PK by physically associating with it by sliding to an adjacent position along the DNA.

## Results

### *Purification and characterization of DNA-PK and Ku*

High salt nuclear extracts that contain both Ku and DNA-PK were fractionated on DEAE–cellulose and sub-

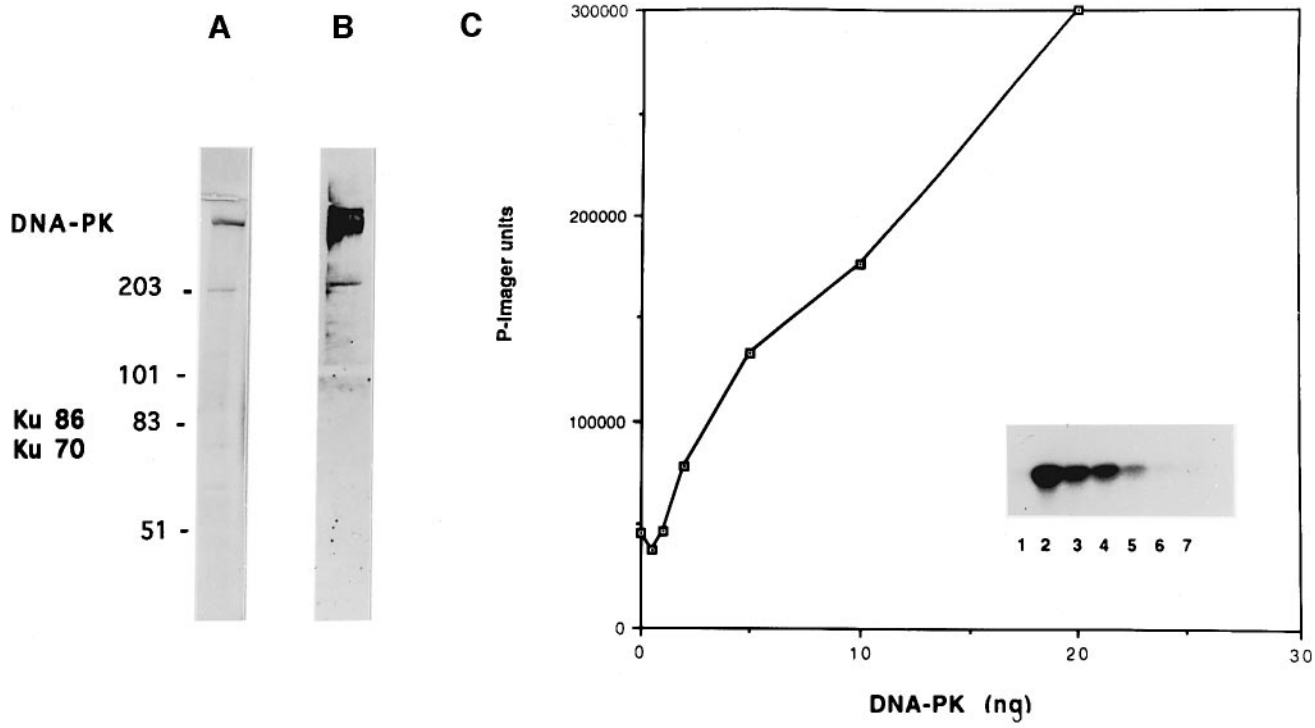


**Fig. 1.** Analysis of the purified DNA-PK preparation. DNA-PK purified from HeLa cells according to the method of Chan *et al*. (1996) was analyzed by: (**A**) SDS electrophoresis; the gel was stained with Coomassie; (**B**) Western blotting using a mixture of anti-DNA-PK monoclonal antibodies 25-4, 18-2 and 42-27 (top portion of the gel) and a mixture of anti-Ku monoclonal antibodies D6D8, RZ2, D6D9 and anti-p70 (bottom portion of the gel); and (**C**) phosphorylation of casein as a substrate. The kinase assay was performed for 10 min at 37°C and the phosphorylated protein was analyzed by SDS electrophoresis in 10% PAG. The gel was dried and exposed. Insert: lane 1, no DNA; lanes 2–7, 20, 10, 5, 2, 1 and 0.5 ng of DNA-PK corresponding to 42, 21, 10, 4, 2 and 1 fmol.

sequently on phosphocellulose columns (Carter *et al*., 1990). The last step of purification involved gel filtration chromatography on a Superose 6 column in the presence of 0.4 M KCl. With this purification method (designated method A), Ku and DNA-PK are dissociated with the peaks of elution at the position of the 150 kDa and 440 kDa markers, respectively. No Ku or DNA-PK was found in fractions with a molecular weight >470 kDa (data not shown).

We were interested in how DNA-PK and Ku might fractionate using a second purification method. DNA-PK and Ku were separated and purified according to the procedure described recently (Chan *et al*., 1996) which involves several ion exchange column chromatographies (designated method B). The last step of purification on a MonoS column completely separated the two proteins. Under these experimental conditions DNA-PK bound to the column, while Ku did not and remained in the flow-through as reported by Chan *et al*. (1996). DNA-PK preparations from methods A and B were analyzed for the presence of Ku using crosslinking to DNA (see below).

Based on its high molecular weight (Figure 1A), reactivity with the antibodies (Figure 1B), and the DNA-dependent kinase activity (Figure 1C), the major band staining with Coomassie (Figure 1A) represents the purified DNA-PK. We could not detect Ku polypeptides in the most purified fraction corresponding to the kinase activity of DNA-PK prepared with method A or B, but this could be due to the limited sensitivity of the immunoblot assay (see below). Quantitation of the phosphorylation of casein by DNA-PK demonstrated that the off-peak fractions of the gel filtration column in method A, which have significantly different levels of Ku, are equally active in stimulation of kinase activity by DNA ends (9-fold activation by DNA) (data not shown). These activities parallel the 470 kDa DNA-PK Coomassie-stained band much better than the bands of Ku. If the kinase activity relied on the equimolar contribution from Ku and DNA-PK, then the peak of kinase activity should be shifted toward the Ku peak. This is not observed in the fractions after MonoQ in method B either. These results raise the possibility that DNA-PK can phosphorylate casein in a DNA-dependent manner in the absence of Ku.

The activity of the purified DNA-PK with undetectable Ku was dependent on the presence of DNA ends, just as is the case for the Ku DNA binding (data not shown). The casein phosphorylation activity of the purified DNA-PK was characterized by time course (data not shown) and dose–response (Figure 1C) curves. The results show that the linear range of this activity is between 5 and 20 min at 37°C, and that this activity is dose-dependent on DNA-PK in a linear manner over a 10 min time course.

The apparent purity of DNA-PK prepared by either method A or B was similar to the apparent purity of the kinase in Figure 1A. No Ku was detected in this preparation of DNA-PK using four specific MAbs for the detection of Ku (Abu-Elheiga and Yaneva, 1992; Wen and Yaneva, 1992); and no DNA-PK in the Ku preparation was detected in immunoblotting using three specific monoclonal antibodies against DNA-PK (Carter *et al*., 1990). The activity of DNA-PK purified by preparation method B was tested using p53 peptide as a phosphorylation substrate and

salmon sperm ds DNA as the co-factor. In these experiments, without any addition of Ku, 10 ng of the kinase was activated by DNA 8- to 12-fold with kinetics similar to those when casein was used as a substrate (Figure 1C). This activity was additionally increased 6-fold in the presence of purified recombinant Ku protein in a dose-dependent manner (data not shown). The latter results are in agreement with the published activation of DNA-PK by Ku (Dvir *et al*., 1993; Chan *et al*., 1996).

### *UV-photoactivated crosslinking demonstrates that DNA-PK can bind directly to linear DNA*

Binding of DNA-PK to DNA was assayed by protein–DNA UV crosslinking. A DNA fragment of 18 bp was used in these experiments, which is smaller than the reported 20–30 bp covered upon binding of Ku to DNA (deVries *et al*., 1989; Knuth *et al*., 1990; Gottlieb and Jackson, 1993). A photoreactive chromophore (5-IdU) in place of T was introduced 1 nt from each end of this ds DNA fragment within the 2 and 3 nt 5′ overhangs at the two respective DNA termini. This photoreactive chromophore is capable of crosslinking the DNA to a protein that binds to DNA upon irradiation with long-wave UV light (Willis *et al*., 1993; Stump and Hall, 1995). In a series of experiments, the time course, specificity and the efficiency of crosslinking at different molar ratios of protein to DNA were determined. Thus, at a DNA-PK to DNA molar ratio of 4:1, this DNA fragment was crosslinked to the 470 kDa polypeptide as well as to small amounts of a 70 kDa polypeptide in the purified fractions of DNA-PK generated by method A (data not shown). At the same molar ratio and conditions for the crosslinking reaction, bovine serum albumin was not crosslinked to this DNA fragment (Figure 2B). (As an additional control protein, no crosslinking of the DNA to purified IgM molecules was observed; data not shown.) These results indicated the presence of a 70 kDa polypeptide in the purified DNA-PK fractions (method A) that could be the p70 subunit of Ku, present at levels below Western blot detectability. However, the ratio between the 470 and 70 kDa crosslinked species in the fractions from the gel filtration chromatography varied from 1.4 to 5.0, suggesting that the two polypeptides crosslinked to DNA quite independently rather than in the type of fixed ratio predictable if Ku and DNA-PK were in a complex.

We were interested in using the UV crosslinking of Ku to DNA as an assay for detection of levels of Ku considerably below Western blot detectability. The trace levels of Ku70 present in the DNA-PK prepared by methods A and B were determined by first establishing a standard curve between the amount of purified recombinant or native Ku and the amount of labeled 18-mer that crosslinks to the 70 kDa subunit (data not shown). Using this standard curve, we could detect levels of Ku at least 30-fold below what we could detect by Western blots. With this method, we could place clear upper limits on the amount of any contaminating Ku in our purified DNA-PK preparations. For purified DNA-PK from preparation method A, the molar ratio DNA-PK/Ku70 is at least 25:1. In DNA-PK samples purified according to method B (Chan *et al*., 1996), no detectable Ku70 was crosslinked to DNA (this enzyme was used in the experiment described in Figure 3 below). Based on the amount of DNA-PK immobilized on the beads and the lack of any detectable Ku70 by the highly sensitive crosslinking method, the molar ratio of DNA-PK to Ku is at least 110:1, and may be much greater (method B).

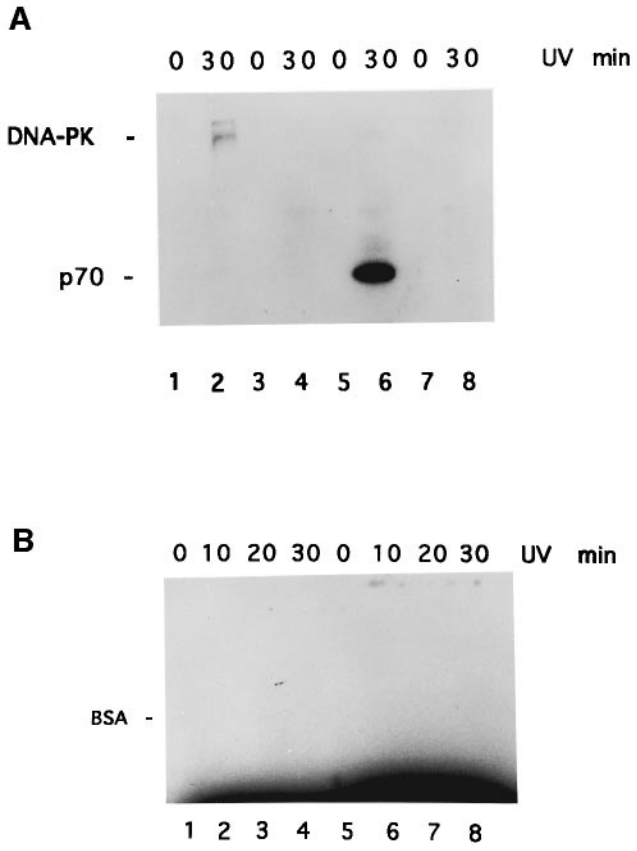


**Fig. 2.** Products of photocrosslinking of DNA to DNA-PK and Ku. (**A**) 20 µl of protein G beads (Sigma) were mixed with 200 µl of cell culture supernatant from hybridomas secreting anti-DNA-PK antibodies. Monoclonal antibodies used were as follows: MAb 42-27 plus 25-4 (lanes 1 and 2); MAb 18-2 (lanes 3 and 4); anti-Ku MAbs (lanes 5 and 6); or anti-c-myc MAb as a control (lanes 7 and 8). The antibodies bound to the beads overnight at 4°C with stirring. These beads were washed three times with 1 ml of 10 mM Tris–HCl, pH 7.5, 0.15 M NaCl, 0.02% Tween-20, and mixed with 50 µl of a partially purified DNA-PK fraction containing ~100 µg protein (fraction before the last step for purification by gel filtration in method A). After incubation for 90 min at 4°C with stirring, the beads were washed three times with 1 ml of kinase buffer containing 0.5 M NaCl, 0.1% NP-40, twice with 1 ml kinase buffer only, and mixed with 62 fmol [$^{32}$P]IdU DNA fragment. (**B**) Control protein (BSA) was mixed with the same [$^{32}$P]IdU DNA fragment at 4:1 (lanes 1–4) and 1:1 (lanes 5–8) molar ratios of protein to DNA and subjected to crosslinking as the immunoimmobilized proteins. The crosslinking of DNA to the proteins was performed as described in Materials and methods. The products of crosslinking were separated by electrophoresis on 8% SDS gel. The gel was dried and exposed to a Kodak film. The apparent band above DNA-PK in (A) is actually the interface between the stacking and resolving portions of the gel. It is important to note that the parallel immunoblots verify the identity of the bands labeled DNA-PK and Ku (not shown).

To determine whether the 470 kDa polypeptide of DNA-PK binds directly to DNA in the absence of Ku, DNA-PK (method A) was additionally purified on immunobeads and assayed for binding to DNA by crosslinking. Protein G beads were loaded with monoclonal antibodies specific for DNA-PK, Ku, or c-myc as a control, and then reacted with the antigens in the fraction applied to the Superose

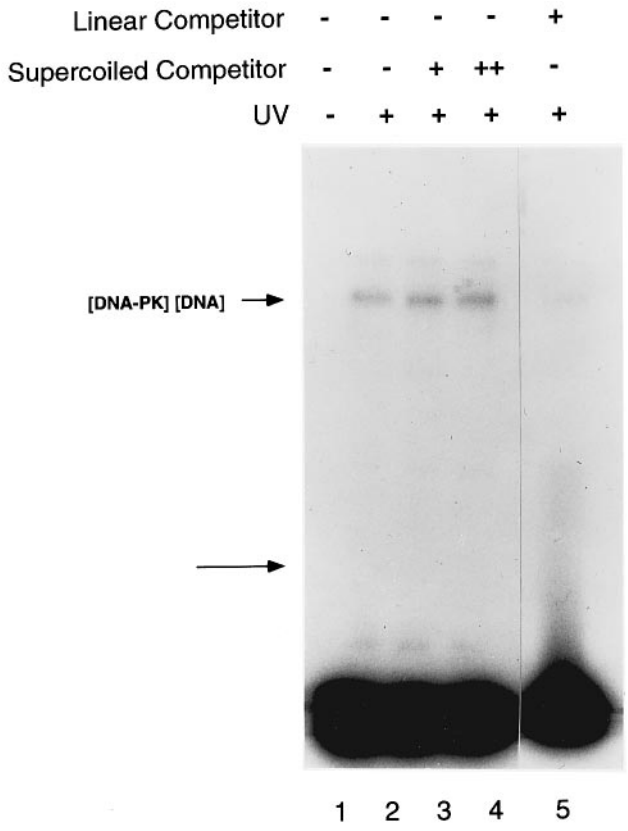


**Fig. 3.** Linear but not supercoiled DNA competes for DNA-PK binding to DNA. 25 ng (52 fmol) of DNA-PK purified by method B was incubated with 0.16 ng (12 fmol) of iodinated $^{32}$P-labeled 18 bp oligonucleotide in the absence (lane 2) or presence of 1.6 ng (lane 3) or 16 ng (lane 4) of supercoiled plasmid DNA designated SD23 (similar results were obtained with other plasmids). The crosslinking was performed for 30 min on ice as described in Materials and methods. Lane 1, DNA-PK with the labeled oligomer before the crosslinking with UV irradiation; lane 5, DNA-PK crosslinking to the labeled oligonucleotide is reduced in the presence of 100 ng unlabeled 79 bp oligonucleotide. The lower arrow indicates the position of the 70 kDa marker; the absence of any crosslinked band at this position indicates that there is no Ku contributing to the binding of DNA-PK to the DNA.

6 column. The immobilized immune complexes were then washed extensively with buffer containing 0.5 M NaCl/0.1% NP-40 to dissociate Ku protein that could be bound to DNA-PK immunobeads. This buffer separates Ku from DNA-PK as shown previously (Suwa *et al*., 1994). Using the crosslinking method described above to detect Ku, we determined that this high salt wash can remove >99.5% of contaminating Ku. Radioactive 18 bp IdU-DNA fragment was subsequently added to each sample at levels such that the proteins were in molar excess. DNA was allowed to interact with the immobilized proteins and then irradiated with UV light for crosslinking. The analysis of the radioactive crosslinked products showed that the 470 kDa polypeptide was bound to DNA on the DNA-PK immunobeads in the absence of the p70 polypeptide (Figure 2A, lane 2). The reactivity of the crosslinked high-molecular weight protein band with monoclonal antibodies in immunoblotting confirmed its identity as DNA-PK. Ku70 could be seen only on the Ku immunobeads (Figure 2A, lane 6). The IgG molecules that are also present on the irradiated beads did not crosslink to DNA; this serves as an internal negative control. These results indicate that DNA-PK can directly contact DNA independently of Ku. Moreover, the absence of crosslinking to Ku70 in the binding reaction (Figure 2A, lane 2) indicates that the DNA-PK crosslinking to DNA is in the absence of Ku.

To confirm that the crosslinking of DNA-PK to DNA was specific for the kinase, DNA-PK was immobilized on immunobeads loaded with monoclonal antibody 18-2 (Carter *et al*., 1990). It has been reported that this antibody inhibits DNA-PK activity, possibly by interference with the DNA binding (Carter *et al*., 1990). Consistent with this hypothesis, no crosslinking of DNA to 470 kDa polypeptide was observed (Figure 2A, lanes 3 and 4). In a control experiment, the 470 kDa polypeptide was detected on these immunobeads by immunoblotting at a level comparable with the one on the beads with the other antibodies (not shown). Therefore, all three IgG1 monoclonal antibodies bind the DNA-PK to the beads, but only the antibody that inhibits DNA binding by DNA-PK also inhibits crosslinking of the 18-mer to the DNA-PK. These results demonstrate that DNA-PK can interact with DNA directly in the absence of Ku protein. In addition, this 18 bp DNA fragment directly stimulated the phosphorylation of casein by the DNA-PK immobilized on the immunobeads with non-inhibitory monoclonal antibodies (42-27 and 25-4) (not shown). Therefore, the association of DNA-PK with DNA is highly specific and can be inhibited by specific monoclonal antibodies that affect DNA binding, but not by other monoclonal antibodies to DNA-PK.

The binding of DNA-PK to the 18 bp ds DNA was not competed by 10- or 100-fold mass excess of negatively supercoiled DNA (Figure 3, lane 2 versus lanes 3 and 4), whereas unlabeled linear DNA effectively competed for DNA-PK binding to the labeled 18-mer (Figure 3, lane 5). This indicates that DNA-PK binding to DNA is directly related to its activity because, like the DNA binding, the DNA-dependent protein kinase activity requires DNA ends, with supercoiled DNA being insufficient.

### *Electrophoretic mobility shift analysis demonstrates direct binding of DNA-PK to linear DNA in the absence of Ku*

The complex between purified DNA-PK (method B) and the 18 bp DNA fragment used in the crosslinking experiments was analyzed also by electrophoretic mobility shift assay. Interestingly, the results clearly show that the DNA-PK can bind directly to the DNA fragment (Figure 4A, lane 6), shifting over 15% of the DNA under these conditions. Moreover, this complex is specifically and fully supershifted in the presence of specific anti-DNA-PK antibody (Figure 4A, lane 7).

The upper limit of contaminating Ku, if any, is less than one part in 110 in the DNA-PK prepared by method B described earlier. In adjacent lanes, purified Ku shifts only ~5% of the 18-mer (Figure 4A, lanes 2–5). Therefore, the maximum amount of contaminating Ku, if any, can only account for ~0.08% of the shifted DNA, whereas >15% of the 18-mer actually shifts when purified DNA-PK is used.

To probe further for any contribution of Ku to the DNA-PK–18-mer complex, either of two purified monoclonal antibodies against Ku were added to see if they caused a

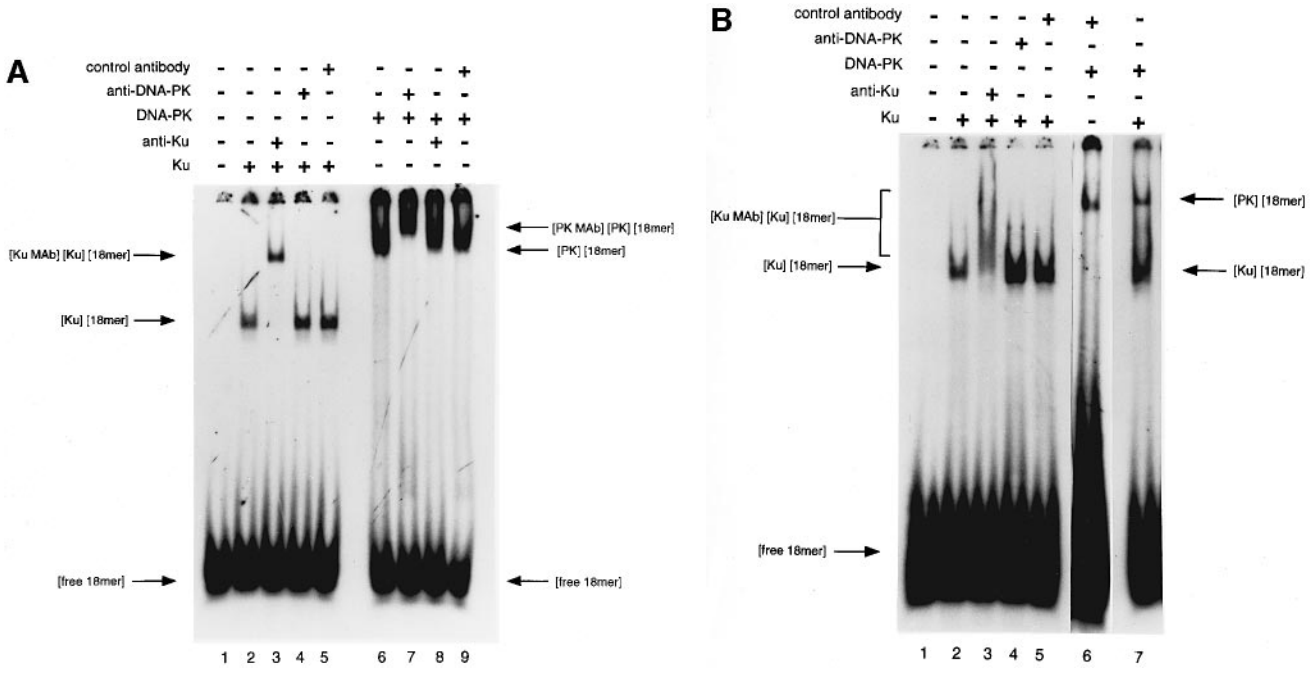


**Fig. 4.** DNA-PK can shift the electrophoretic mobility of DNA in a Ku-independent manner. Purified recombinant Ku (5 ng, 33 fmol) or purified DNA-PK (10 ng, 21 fmol) were incubated in the absence or in the presence of various monoclonal antibodies for 30 min on ice. End-labeled 18 bp DNA fragment (0.4 ng, 30 fmol) was added and the mixtures (total volume 20 µl) were incubated for 15 min at room temperature. DNA–protein complexes were analyzed by electrophoresis in 5% PAGE in 0.5× TBE. (**A**) Lane 1, no protein added; lane 2, Ku–DNA complex; lane 3, Ku–DNA complex supershifted by 0.4 µg anti-Ku MAb 162 (Ku Ab-3, Neomarkers, Inc.); lane 4, Ku–DNA complex in the presence of 1.1 µg of anti-DNA-PK MAb 25-4; lane 5, Ku–DNA complex in the presence of 3 µg control MAb (anti-T-cell receptor); lane 6, DNA-PK–DNA complex; lane 7, DNA-PK–DNA complex supershifted by 1.1 µg anti-DNA-PK MAb 25-4; lane 8, DNA-PK–DNA complex in the presence of 0.4 µg anti-Ku MAb 162; lane 9, DNA-PK–DNA complex in the presence of 3 µg control MAb (anti-T-cell receptor). (**B**) Lane 1, no protein added; lane 2, Ku–DNA complex; lane 3, Ku–DNA complex supershifted by 0.7 µg anti-Ku MAb D6D8 (Yaneva *et al*., 1985); lane 4, Ku–DNA complex in the presence of 1.1 µg anti-DNA-PK MAb 25-4; lane 5, Ku–DNA complex in the presence of 3 µg control MAb (anti-T-cell receptor); lane 6, DNA-PK–DNA complex; lane 7, Ku (5 ng, 33 fmol) and DNA-PK (10 ng, 21 fmol) incubated with DNA. Lane 6 was exposed to film longer to illustrate clearly the position of the DNA-PK–DNA complex.

supershift of the DNA-PK–Ku complex. Neither one shifted the DNA-PK–DNA complex (Figure 4A, lane 8), yielding the same result as the lane with the sample treated with the control antibody (Figure 4A, lane 9) or the lane with no antibody (Figure 4A, lane 6).

As is well known, recombinant Ku also gives a discrete mobility shift (Figure 4A, lane 1); native Ku behaves identically (deVries *et al*., 1989; Zhang and Yaneva, 1992; Wu and Lieber, 1996). Because the 18-mer is small, only one Ku70/86 can load; with longer ds DNA fragments, one observes multiple shifted species. A specific anti-Ku monoclonal antibody supershifts the Ku–DNA complex (Figure 4A, lane 3).

When a 1.6-fold molar excess of recombinant Ku was mixed with DNA-PK and the 18-mer, only the Ku and DNA-PK individual complexes were observed. There was clearly no evidence of a Ku–DNA-PK–DNA complex (Figure 4B, compare lane 7 with lanes 1, 3, 5 and 6). This experiment used a different anti-Ku monoclonal antibody from that used in Figure 4A, and this antibody causes a smeared supershift of Ku. Nevertheless, the conclusion is clear: DNA-PK and Ku form independent complexes with 18 bp linear ds DNA.

### *Activity of DNA-PK immobilized on immunobeads*

To illustrate further the separability of Ku and DNA-PK for DNA-dependent protein kinase activity, purified DNA-PK (method A) was treated with protein G beads with pre-bound monoclonal anti-Ku antibodies or pre-bound anti-DNA-PK monoclonal antibodies, and the kinase activity was assayed for phosphorylation of casein or synthetic p53 peptide. As controls, monoclonal antibodies specific for c-myc were bound first to protein G beads. The beads were washed, and then 120 ng of purified DNA-PK (0.25 pmol) were added to each of the immunobead preparations for interaction with the antibodies. The kinase activities on these immunobeads and the supernatants after binding were determined using the casein assay. The results showed that the enzyme bound to the DNA-PK immunobeads was activated 6-fold by DNA; this was similar to the activity in the initial kinase preparation that was activated 7-fold (Figure 5A, compare lanes 1 and 2 with lanes 11 and 12). The beads with anti-Ku antibodies had a minimal kinase activity (Figure 5A, lanes 9 and 10). The supernatant depleted of DNA-PK by the anti-DNA-PK beads had a much lower level of activity (Figure 5A, lanes 7 and 8) than before depletion (Figure 5A, lanes 1 and 2). The supernatant after treatment with anti-Ku beads (Figure 5A, lanes 3 and 4) had activity as in the control supernatant treated with anti-c-myc beads (Figure 5A, lanes 5 and 6). It should be noted that the beads were loaded with three different MAbs against Ku86, plus one against Ku70, ensuring the binding of Ku to the beads if Ku had been present in association with DNA-PK. These results indicate that the large majority, if not all, of the DNA-dependent kinase activity can be accounted for by DNA-PK alone, in the absence of Ku.

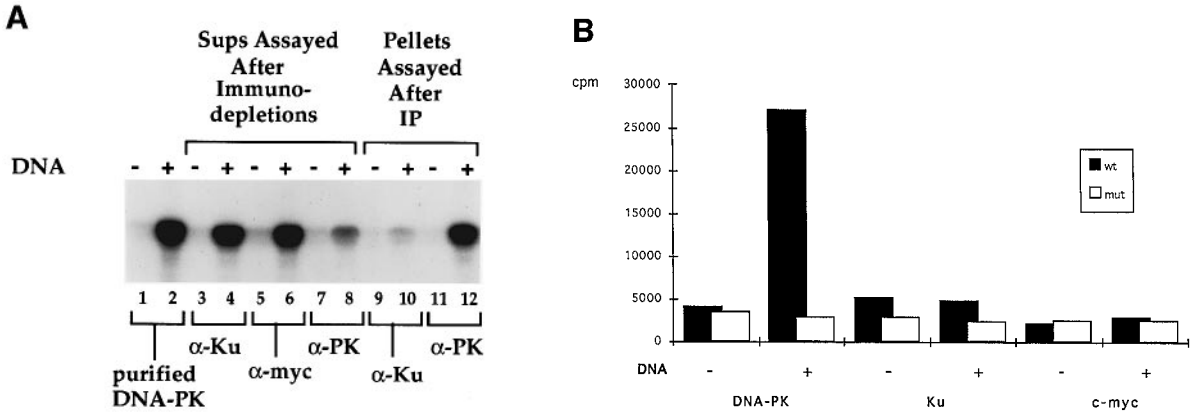


**Fig. 5.** Effect of immunodepletion of Ku from a DNA-PK preparation on the activity of the kinase. The immunoimmobilized DNA-PK described in Figure 2 was analyzed for kinase activity. The kinase assay was performed for 10 min at 37°C in the absence (–) or presence (+) of DNA. (**A**) Phosphorylation of casein. Lanes 1 and 2, using 10 ng (21 fmol) of partially purified DNA-PK as a positive control; lanes 3–8 and 9–12 are immunodepletions. 10 μl of supernatant after incubation with anti-Ku immunobeads (lanes 3 and 4; three anti-Ku86 and one anti-Ku70 MAbs were loaded onto the beads), control antibody (anti-myc) immunobeads (lanes 5 and 6), or anti-DNA-PK immunobeads (lanes 7 and 8) were assayed for phosphorylation of casein in the presence of salmon sperm DNA. Lanes 9 and 10, phosphorylation from activity retained by anti-Ku immunobeads; lanes 11 and 12, phosphorylation by activity retained by anti-DNA-PK immunobeads. The fold stimulation by DNA was quantitated using a phosphorimager. (**B**) Phosphorylation of p53 peptide. The beads with the immunoimmobilized proteins were washed with 0.5 M KCl-containing buffer, followed by two washes with kinase buffer, and 5 μl of the beads suspension were assayed for phosphorylation of the p53 synthetic peptide as described previously (Finnie *et al*., 1995).

The above results were obtained using casein as the phosphorylation target. The immunobeads from the experiments described above also were tested for phosphorylation of p53 peptide as described (Lees-Miller *et al*., 1992). Phosphorylation of the wild-type peptide was activated >10-fold by DNA when immunobeads with bound DNA-PK were used compared with a 2-fold activation when immunobeads with Ku were used (Figure 5B). These results show again that Ku is not required for the activation of DNA-PK by DNA. In addition to casein, p53 peptide can be phosphorylated by DNA-PK also in the absence of Ku protein.

### *Stimulation of DNA-PK by Ku requires DNA that is long enough for separate binding by DNA-PK and Ku*

Previous studies have shown that Ku stimulates DNA-PK activity. We were interested in determining if this stimulation was dependent on the length of the DNA. Using the 18 bp ds oligonucleotide fragment described above to stimulate purified DNA-PK (containing less than one part in 110 of contaminating Ku), we find no stimulation of the already active DNA-PK when we add purified native or recombinant Ku at nanomolar concentrations. In contrast, when we use salmon sperm DNA sheared to an average size of 2 kb, we find that Ku is able to stimulate DNA-PK up to 8-fold at similar concentrations (data not shown). This is consistent with the level of stimulation that others have seen using purified DNA-PK and Ku (Chan *et al*., 1996). Therefore, Ku can stimulate DNA-PK when the DNA fragment is sufficiently long to allow binding of both Ku and DNA-PK to the same fragment, but not when that length is inadequate.

### *Analysis of the interaction between DNA-PK and DNA by atomic-force microscopy: DNA-PK and Ku can be distinguished based on their apparent size*

Images of Ku, DNA-PK and of the mixture of both proteins are shown in Figure 6A–C. Due to the substantial difference in size (152 kDa for Ku versus 470 kDa for DNA-PK) both proteins could be visually distinguished on the atomic-force microscopy (AFM) topographs. Those differences were clearly reflected in distributions of sizes of individual molecules, as illustrated on volume histograms in Figure 6D–F.

The apparent volumes of individual molecules exceeded the values predicted from molecular weights of both proteins (193 $nm^3$ for Ku and 581 $nm^3$ for DNA-PK) assuming the typical density of 1.34 $g/cm^3$ (Cantor and Schimmel, 1980). This discrepancy is caused by the finite size of the AFM tip (Keller, 1991; Williams *et al*., 1996). (The typical radius of silicon-etched tips used throughout this study was in the range 10–20 nm, which is comparable with a size of a single protein molecule.)

Mean apparent heights observed for both proteins (1.1–1.5 nm for Ku and 2.0–2.5 nm for DNA-PK, distributions not shown) were smaller than estimated for the globular protein based on molecular weights. Such discrepancies are commonly observed in AFM imaging of proteins adsorbed on mica (Shao *et al*., 1995). Typical explanations of this effect invoke conformational changes upon adsorption, and relative differences in mechanical and surface properties between the mica substrate and protein molecule (Bustamante and Rivetti, 1996). In this study we did not observe any significant dependence of apparent height of the same protein molecule imaged under different cantilever oscillation amplitudes and different setpoints, and thus we favor the explanation based on conformational changes.

The geometrical effect of the finite size of an AFM tip and the observed distribution of heights of individual protein molecules (reflecting different extents of flattening upon adsorption) allowed us to explain the observed shape of distributions of apparent volumes. Simple geometrical considerations indicate that the magnitude of tip-size contribution to the apparent volume of an object increases with its height. More detailed analysis (data not shown) indeed revealed a nearly linear relationship between the

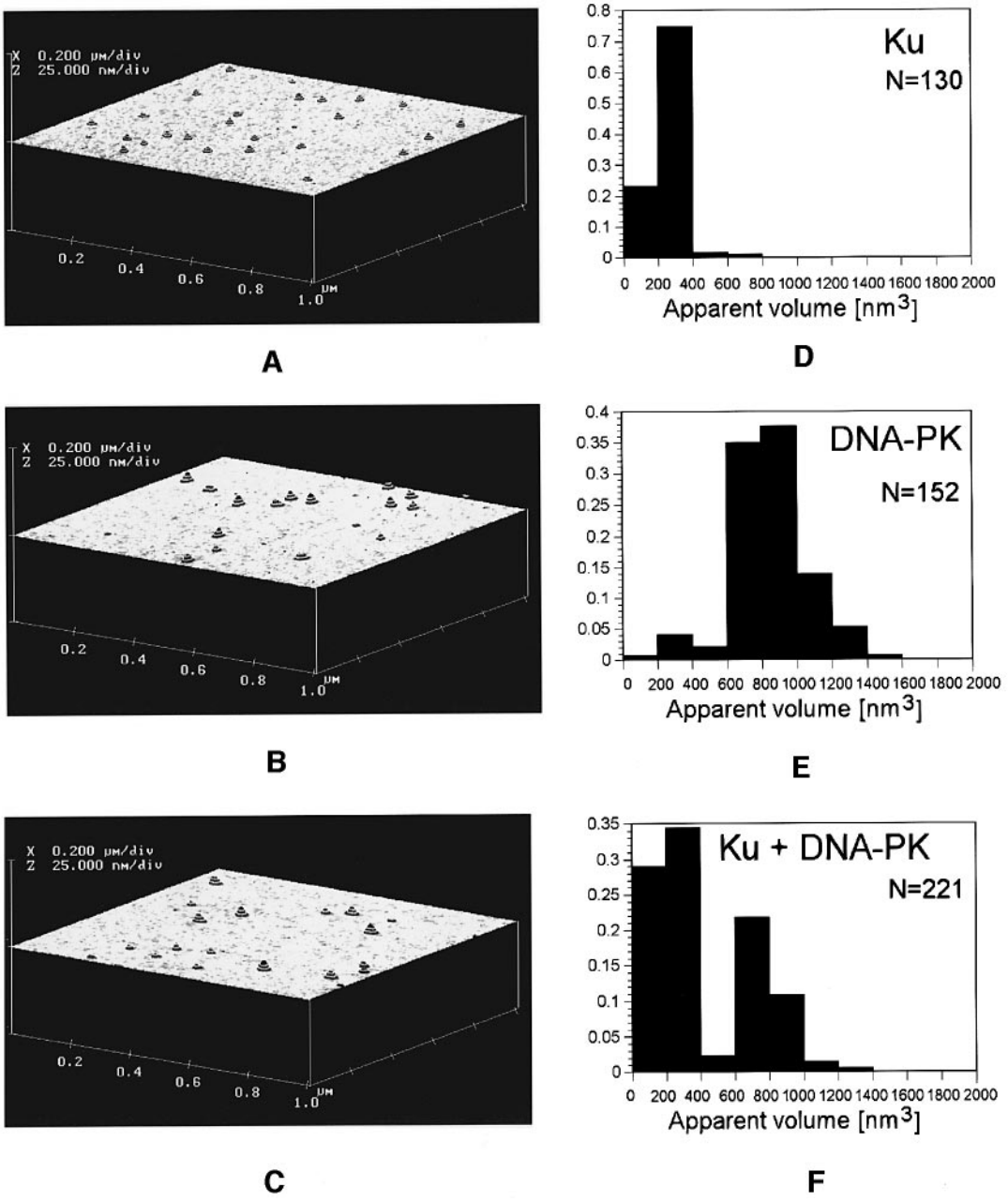


**Fig. 6.** Tapping mode AFM topographs and histograms of apparent volumes of Ku, DNA-PK and of the mixture of both proteins adsorbed on the surface of mica (scan area 1 μm×1 μm). The DNA-PK used in the AFM study was purified by method B, in which Ku was quantitated to be <1 molecule per 110 molecules of DNA-PK. Ku was prepared as a recombinant protein using a baculovirus expression system. (**A**–**C**) AFM topographs in this and subsequent figures are presented in three-dimensional renderings. In order to aid in visualization of the elevation of features, the height was coded with a periodic gray scale. Protein concentrations in solutions used for deposition: (A) [Ku] = 12 nM; (B) [DNA-PK] = 1.7 nM; (C) [Ku] = 6 nM, [DNA-PK] =0.85 nM. (**D**–**F**) Histograms of apparent volume of three-dimensional surface features observed in the AFM topographs of Ku (D), DNA-PK (E) and of the mixture of both proteins (F) adsorbed on the surface of mica. Both proteins are clearly distinguishable based on their apparent volume. Notice the ~5% fraction of features with volumes between 200 and 400 $nm^3$ in the histogram of DNA-PK. We believe that this fraction corresponds to breakdown products of DNA-PK.

volume and height of individual molecules imaged with the same probe. Comparison of data sets acquired with different probes revealed some variability in the slope and offset of volume–height relationships, pointing to variability in probe radius.

Based on these results, we concluded that the distributions of volumes primarily reflected the distribution of orientations and conformations of individual protein molecules on the surface and were additionally broadened due to variability of the radius of the AFM probe.

### *AFM-visualized interactions between DNA and Ku*

The tapping mode AFM image of 841 bp DNA adsorbed on mica is shown in Figure 7. The lengths of most DNA chains observed in AFM topographs were consistent with the length expected for an 841 bp double helix with a rise of 3.4 Å per base pair. A small fraction of shorter chains was also typically present (not shown), pointing to some fragmentation of DNA chains in the course of sample preparation.

When Ku and the 841 bp fragment were mixed together,

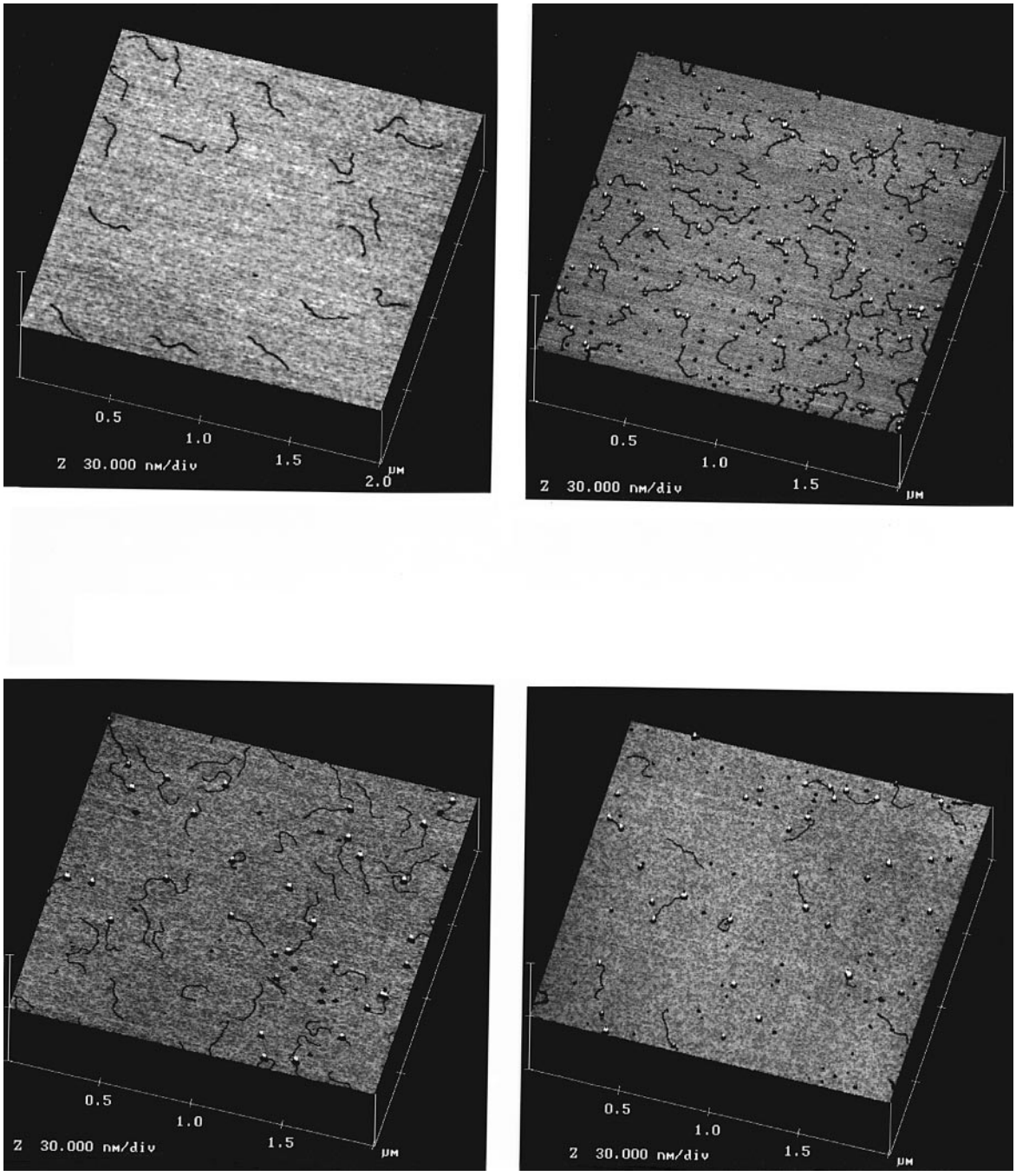


**Fig. 7.** Tapping mode AFM topographs of 841 bp DNA and mixtures of DNA with proteins adsorbed on the surface of mica. Scan area 2 μm×2 μm. The contrast and offset of the periodic gray scale coding for height was adjusted to the settings which provided optimum contrast in the images of DNA–protein complexes shown below. In this representation DNA chains appear as black features on the gray background of mica. Upper left panel, DNA; upper right, DNA + Ku; lower left, DNA + DNA-PK; lower right, DNA + DNA-PK + Ku. In all cases a substantial amount of protein(s) appears to be associated with DNA chains. Notice the clear preference of DNA-PK towards the DNA ends, and lack of such preference in the case of complexes of Ku with DNA. Protein and DNA concentrations in solutions used for deposition: upper right panel: [Ku] = 44 nM, [DNA] = 0.78 nM; lower left: [DNA-PK] = 1 nM, [DNA] = 0.15 nM; lower right: [DNA-PK] = 1 nM, [Ku] = 6 nM, [DNA] = 0.15 nM.

isolated Ku molecules distributed at sporadic positions along the length of each ds DNA fragment. A substantial fraction of the Ku molecules bound to the DNA ends, but many other Ku molecules also assumed internal positions (Figure 7). When we lengthened the incubation time or increased the concentration of Ku from 6 nM to 44 nM, higher percentages of the Ku migrated to internal positions on each fragment (data not shown), confirming previous observations (deVries *et al*., 1989). The apparent volume of DNA-bound Ku was somewhat larger than that of 'free' Ku molecules. We believe that this reflects the increase of elevation of DNA-bound protein above the surface of mica and/or the increased resistance to protein flattening upon DNA binding.

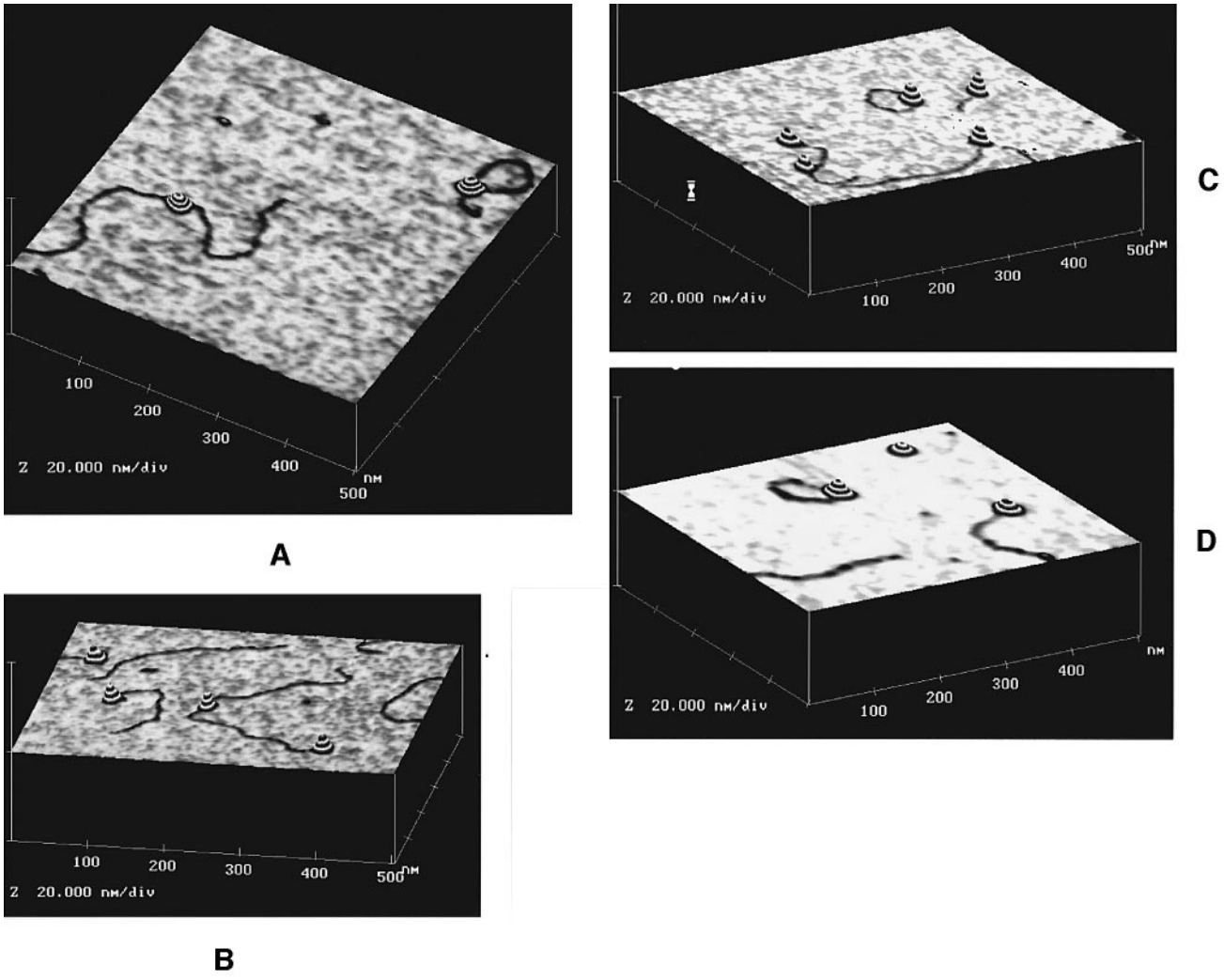


**Fig. 8.** Tapping mode AFM topographs of complexes of DNA-PK with DNA. The 'dimers' of DNA created by binding of two separate DNA chains to the same DNA-PK molecule (**A**, left; **B**, center) were frequently observed. Unambiguous identification of such complexes as 'dimers', as opposed to longer chains with the protein bound in the center, was made possible by using monodisperse, 841 bp DNA throughout the study. The circular DNA–protein complexes, such as those shown in (A), (**C**) and (**D**) were observed sporadically. (500 nm×500 nm images, zoomed-in from 2 μm×2 μm scans, protein and DNA concentrations as in Figure 7.)

### *AFM-visualized interactions between DNA and DNA-PK in the absence of Ku*

AFM experiments confirmed our biochemical observations that DNA-PK directly binds and is activated by DNA termini (Figures 2, 4 and 5). Images of mixtures of DNA-PK with 841 bp DNA fragment revealed a very high incidence of DNA–protein complexes (Figures 7 and 8A–D). The most striking feature of those was the preferential association of DNA-PK with DNA ends (in >84% of cases). Another interesting feature was the frequent occurrence of dimers (Figure 8A and B) and (less frequently) circular forms of DNA chains (Figure 8A, C and D) conjoined by a DNA-PK molecule at the junction. The 841 bp fragment alone showed no evidence of end-to-end association either between fragments or through circularization (Figure 7).

As in the case of Ku–DNA complexes, the apparent volume of DNA-PK associated with DNA ends was larger than the apparent volume of 'free' DNA-PK (data not shown). We propose a similar explanation for this effect (increase of elevation of DNA-bound protein above mica and/or the increased resistance to protein flattening).

### *Pre-saturation of DNA-PK with 18-mer ds DNA blocks its binding with the 841 bp DNA fragment*

We have suppressed the ability of DNA-PK to bind the 841 bp fragment by pre-incubation with an excess of 18 bp DNA (data not shown). This is an important technical point because it indicates that, in crude mixtures that contain nucleic acid fragments, the binding properties of DNA-PK may be affected. Purification steps such as anion exchange columns are usually necessary to remove the nucleic acids.

### *AFM-visualized interactions between DNA and mixtures of Ku and DNA-PK*

When DNA-PK and Ku were both incubated with the 841 bp DNA fragment, we have also observed formation of protein–DNA complexes which, based on their apparent size, resembled those formed in binary mixtures (Figure 7 and Figure 9A–D). As previously, isolated Ku molecules were distributed along DNA whereas DNA-PK exhibited a clear preference towards the ends of DNA molecules. Inspection of the distribution of apparent volumes of the larger of the two proteins revealed, however, a significant

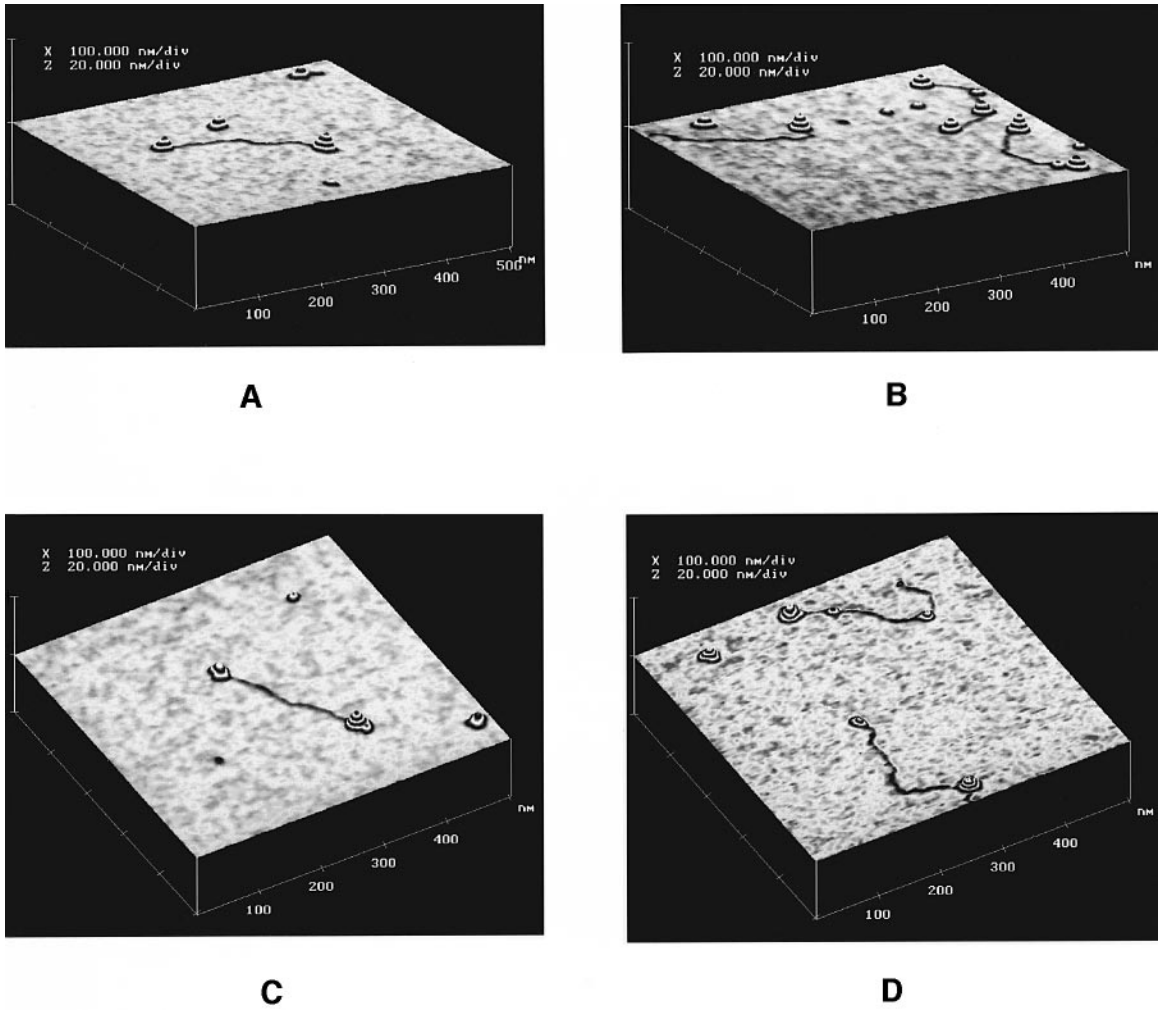


**Fig. 9.** Tapping mode AFM topographs of complexes formed from solution of DNA with both Ku and DNA-PK. Complexes of DNA-PK and Ku with DNA resembled closely those observed in single-protein samples. In addition a significant fraction of abnormally large DNA end-bound complexes (**A**, right and **C**, right; compare with **A**, left and **C**, left) was observed. (500 nm×500 nm images, zoomed-in from 2 μm×2 μm scans.) Concentrations of proteins and DNA are the same as in Figure 7.

broadening towards higher values compared with DNA-PK alone on DNA. We propose that those larger species were ternary complexes of DNA, DNA-PK and Ku. Examples of such abnormally large complexes side-by-side with DNA-bound DNA-PK are shown in Figure 9A and C. With few exceptions, when Ku and DNA-PK could be resolved (Figure 9C), most DNA-PK–Ku complexes were featureless, and only their abnormally large volume pointed to the presence of two proteins.

Further indications about the nature of ternary complexes were provided by geometrical analysis involving comparisons of effective apparent areas of isolated and DNA-bound molecules (Figure 10A and B). The apparent effective (abbreviated aeff) area of a molecule, $S_{aeff}$ was defined for the purpose of this comparison as a ratio of apparent volume to height. In the absence of Ku, the distributions of effective areas of isolated and DNA-bound DNA-PK were almost indistinguishable (Figure 10A). In contrast, in the presence of Ku, the distribution corresponding to bound DNA-PK was significantly shifted towards higher values (Figure 10B). This means that the abnormally large volume of species identified as DNA-PK–Ku complexes was caused mainly by the increase of their lateral size. As illustrated in the model in Figure 11, comparison of the effective area of a 'complex' of two objects and the effective areas of its components provides information about the global configuration of a complex. Hence, we propose that the observed relationship $S_{aeff}$ (DNA-PK–Ku) $>$ $S_{aeff}$ (DNA-PK) indicates that in complexes, DNA-PK and Ku assumed adjacent positions along the DNA chain.

## Discussion

### *DNA end binding by DNA-PK and the effect of Ku on DNA-PK activity*

These studies provide novel insights into several aspects of the function of DNA-PK. First, DNA-PK can bind directly to DNA, as demonstrated by crosslinking (Figures 2 and 3) and electrophoretic mobility shift assays (Figure 4). A monoclonal antibody against DNA-PK that interferes with DNA binding prevents the crosslinking (Figure 2) and the kinase activation (Carter *et al*., 1990), while two other monoclonal antibodies against DNA-PK do not affect DNA binding and also do not affect crosslinking or kinase activity (Carter *et al*., 1990). Second, DNA binding by DNA-PK has a functional effect; kinase activity

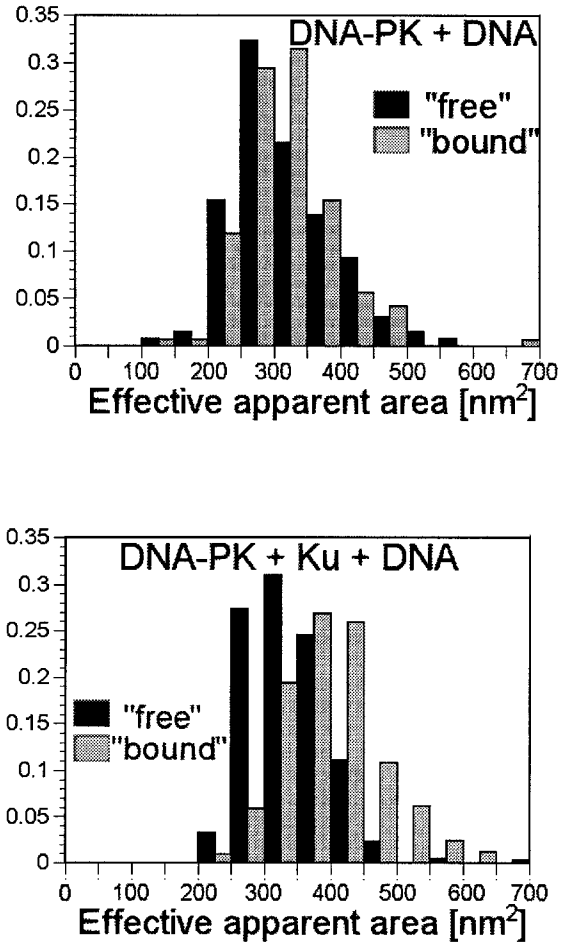


**Fig. 10.** Histograms of apparent effective areas. Effective areas, defined as a ratio of apparent volume to apparent height, of 'free' and 'bound' DNA-PK (**A**) and DNA-PK + Ku (**B**). This comparison indicates that the higher apparent volume of DNA–DNA-PK–Ku complexes results primarily from the increase of lateral size (see also Figure 11). (Objects below 400 $nm^3$ have been excluded from consideration.)

is stimulated by the same small 18 bp oligonucleotide to which it also crosslinks and mobility shifts. Third, Ku binds separately to DNA. This is illustrated by the distinct mobility shift species for DNA-PK versus Ku (Figure 4B), documented with immunodepletion experiments and supershifts of each protein. The functional significance of this separate DNA binding is borne out by comparing the kinase activity with and without Ku when using short DNA. The 18-mer is too short to allow both Ku and DNA-PK to bind to it, as illustrated by the mobility shift studies (Figure 4). The activation of DNA-PK by the 18-mer is quite effective; however, the DNA-PK complexed with the 18-mer cannot be stimulated by Ku. Addition of Ku protein to phosphorylation reactions did not increase the activity of the kinase when it was activated by the 18 bp DNA. This is consistent with the possibility that this fragment may be too small to permit simultaneous binding by both Ku and DNA-PK. The footprint of Ku alone has been determined to be 20–30 bp (Mimori and Hardin, 1986; deVries *et al*., 1989; Knuth *et al*., 1990). It is important to note that longer DNA [such as oligos that are over 80 bp (M.Yaneva, R.West and M.Lieber, manuscript in preparation) or sheared calf thymus DNA] is able to stimulate DNA-PK as the 18-mer, but in these cases the presence of Ku provides additional stimulation.

The picture that emerges from these studies is that DNA-PK and Ku bind separately to DNA. Our studies confirm that Ku does stimulate DNA-PK activity up to 8-fold, but only on the long DNA. Collisional interaction is unlikely to explain the Ku stimulation of DNK-PK. If this were the case, the Ku–DNA and DNA-PK–DNA complexes would be able to associate collisionally, resulting in some level of stimulation even when they are on separate molecules, and this clearly does not occur. Therefore, collisional interaction is unlikely to explain the Ku stimulation of DNA-PK. Because Ku is known to translate in an energy-independent fashion along DNA, Ku and DNA-PK may associate after both have independently bound DNA. If the DNA length is too short to permit Ku and DNA-PK to bind to the same DNA molecule, then the stimulation of DNA-PK by Ku fails to occur, as we observed. This indicates that the Ku stimulation of DNA-PK requires that they be physically adjacent to one another along the DNA.

### *DNA-PK and Ku do not form a detectable protein complex and they co-associate by independent binding with linear DNA*

Do Ku and DNA-PK co-purify? Analytically, Ku and PK do not migrate together on a sizing column when analyzed in crude extracts from a high or a low salt extraction. The bulk of the two proteins do not co-migrate; there is only overlap of the Ku and DNA-PK peaks during the purification on ion exchangers. The lack of co-purification is not surprising given that the proteins fail to associate at the crude extract stage (data not shown). In order to designate a protein as having an oligomeric structure, it must be an entity that can be isolated. A search for a physical complex between DNA-PK and Ku in crude extracts did not reveal a significant level of Ku–DNA-PK association; the complex that could be occasionally seen was at the lower detection limits of the methods used, and represented $<5\%$ of the two proteins in solution.

Do Ku and DNA-PK form a complex once each independently loads onto DNA? Based on the data here and in Suwa *et al*. (1994), it appears that the association of Ku and DNA-PK requires linear DNA longer than 18 bp. If short DNA fragments are used (18 bp), then the Ku and DNA-PK associate with independent fragments and cannot take up adjacent positions on the same DNA fragment. When longer DNA fragments are used, then some level of co-immunoprecipitation of Ku and DNA-PK can be seen because antibodies that pull down one protein will pull down the bound DNA along with the other DNA-binding protein. If the association between Ku and DNA-PK is due only to their interaction after they each load onto DNA, such an interaction may be unstable after dissociation from the DNA, explaining why Ku and DNA-PK fail to associate in solution and why genetic searches for their interaction have failed (Wu and Lieber, 1996).

Because such a large fraction of DNA-PK appears not to be associated with Ku, we examined the possibility that DNA-PK may bind to DNA directly in the absence of Ku and may be activated for kinase activity directly by such DNA binding. Our evidence that this is true is as

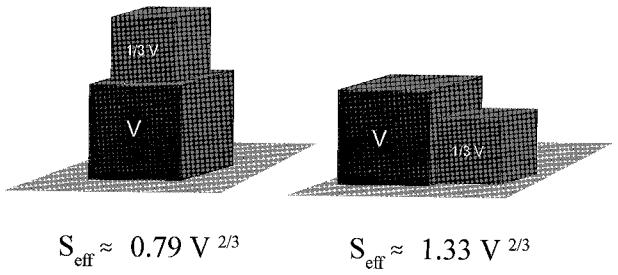


**Fig. 11.** Model illustrating the relationship between the effective area of a complex object and configuration of its components. The model 'complex' consists of two cubes with volumes V and 1/3V (corresponding to the ratio of volumes of DNA-PK and Ku). The effective area of a larger cube is equal to $S_{eff} = V^{2/3}$. Simple calculation shows that in the vertical arrangement (left), the effective area of the 'complex' is ~20% smaller than the effective area of the larger cube, whereas in the lateral arrangement (right) it is about 1.33 times larger. We have observed a similar increase of the effective apparent area of DNA-bound complexes of DNA-PK with Ku in comparison with DNA-PK (see Figure 10). This suggests that, in the complex, DNA-PK and Ku assume adjacent positions on the DNA end.

follows. First, we find that the fold of DNA stimulation of the kinase does not vary as we assay gel filtration fractions from the peak of the 470 kDa polypeptide and compare them with adjacent off-peak fractions that have increasing amounts of Ku. If Ku and DNA-PK combined to form an active complex, then the peak of activity of the putative holoenzyme should be between the peaks of Ku and DNA-PK rather than directly associated with the DNA-PK alone, and this is not the case.

Second, when purified preparations of DNA-PK were crosslinked to an 18 bp ds DNA fragment, only a minor contaminant of Ku was detected for DNA-PK prepared by one method (<1 molecule in 25, method A). DNA-PK purified by a second method (method B) showed no detectable Ku at the level of one molecule in 110. Independently, DNA-PK also crosslinks to the ds DNA. The DNA-PK and the Ku appear to bind and crosslink to the ds DNA fragment independently because the ratio of the two crosslinked products varies (from 1.4 to 5.0 in a series of adjacent gel filtration fractions) rather than remains constant, as we would expect for a specific Ku–DNA-PK complex.

Third, purified DNA-PK was bound to immunobeads and washed with 0.5 M NaCl/0.1% NP-40 to remove any minor contaminating Ku. Crosslinking of the DNA to the 470 kDa DNA-PK was still observed (Figure 2). No Ku crosslinking on these DNA-PK immunobeads in these types of experiments was detected. In parallel, DNA-dependent kinase was active on these immunobeads. The fold stimulation by the DNA in this immobilized system was indistinguishable from the kinase activity of the purified DNA-PK in the aqueous phase before binding to the immunobeads (Figure 5). The latter observation would be inconsistent with even markedly sub-stoichiometric amounts of Ku acting in a catalytic manner to activate multiple DNA-PK molecules sequentially (e.g. by a single Ku molecule diffusing from one DNA-PK to another). If such a mechanism were operating, it would be markedly dependent on diffusional collision frequency of the Ku with the DNA-PK. Thus, one would expect the dependence of kinase stimulation on DNA to be markedly affected if one of the components was diffusionally arrested by immobilization, and it clearly was not. Because we detect no Ku by a highly sensitive crosslinking assay and because the DNA dependence remains unaffected by immobilization of the DNA-PK (Figure 5), it is clear that DNA-PK is binding directly to the 18 bp ds DNA fragment and being stimulated by this DNA in the absence of Ku.

Fourth, electrophoretic mobility shifts demonstrate independent binding of Ku and DNA-PK to an 18 bp ds DNA fragment. Ku forms one complex with the DNA, and DNA-PK forms another. When both Ku and DNA-PK are present, a mixture of the two mobility shift species is present precisely at the mobilities predicted from the binding of the individual Ku and DNA-PK. From these studies, it is clear that an 18 bp ds oligonucleotide is too small a DNA fragment for both Ku and DNA-PK to bind concurrently given that the Ku footprint is 20 to 30 bp (Mimori and Hardin, 1986; deVries *et al*., 1989). At least under the conditions of this electrophoretic mobility shift, DNA-PK and Ku do not form a protein–protein complex.

How does one reconcile the data that we have indicating a lack of interaction between DNA-PK and Ku with data that suggests such an interaction? The model in which Ku and DNA-PK do form an oligomeric complex in which Ku is the DNA-binding domain and DNA-PK is the catalytic domain must be revised to accommodate the data indicating that Ku and DNA-PK independently bind DNA ends. Ku is known to slide along DNA. Therefore, Ku may assume a position adjacent to the DNA-PK, resulting in the 2- to 8-fold stimulation that we and others observe (Finnie *et al*., 1995; Chan and Lees-Miller, 1996). This view would be consistent with all published data indicating a stimulation of DNA-PK by Ku in crude extracts (using the pull-down assay) or in more purified preparations.

The physiological phosphorylation target of DNA-PK is not yet known. Different substrates may be phosphorylated by DNA-PK in different ways. Data using the transcription factor Sp1 as the target indicate no phosphorylation in the absence of Ku (Gottlieb and Jackson, 1993). In contrast, p53 peptide, CTD tail of RNA polymerase II (Dvir *et al*., 1993), RP-A (Brush *et al*., 1994; Pan *et al*., 1994), and casein clearly do not require Ku for phosphorylation by DNA-PK. None of these substrates is known to be the physiologically relevant target of DNA-PK. The distinctive behavior of Sp1 may be because of some interaction between Sp1 and Ku.

Rodent cells have a level of DNA-PK that is 50- to 100-fold lower than human cells (Anderson and Carter, 1996), making complete purification of DNA-PK from rodent cells impractical. We have tried to use the anti-human DNA-PK monoclonal antibodies to capture murine DNA-PK onto immunobeads out of crude extracts. This would have permitted comparison of DNA-PK activity in extracts from wild-type cells and from cells that have a knock-out of both Ku86 alleles. However, the level of DNA-PK that can be captured onto such beads is quite low, perhaps because of the cross-species nature of the antibodies (M.Yaneva, P.Hasty and M.R.Lieber, unpublished results). Hence, the DNA-PK activity measurements on such immunobeads are not reliable.

### *Atomic-force microscopy*

Atomic-force microscopy provided valuable insights into interactions of DNA-PK with DNA. Its major strength in

the described study stemmed from its ability to visualize the global geometry of DNA–protein complexes and to identify the proteins and protein complexes based on their apparent size. In the past, uncertainties in the AFM measurements of sizes of protein molecules adsorbed on solid surfaces (tip-size contribution, conformational changes upon adsorption, deformability of molecules) discouraged the authors from more detailed quantitative analysis. Our studies confirmed that such objections are justified if scarce measurements of one parameter (especially height) are available. However, more labor-intensive analysis of distributions of volumes, typically requiring hundred(s) of individual measurements, proved to be fully informative.

Based on AFM observations we were able to establish unambiguously that DNA-PK binds predominantly to DNA termini. In contrast, Ku was found to distribute along DNA chains (deVries *et al*., 1989). Therefore, the DNA-binding properties of purified DNA-PK appear to be distinct from Ku, which loads from a DNA terminus, but typically slides to internal positions.

End-to-end association of the same DNA fragment or between two fragments is apparent for DNA-PK as well as mixtures of DNA-PK and Ku when added to DNA. Therefore, DNA-PK may have more than one DNA-binding site. These observations may be relevant to the ligation step in double-strand break repair and in V(D)J recombination, and we are currently investigating this possibility.

Interestingly, when Ku and DNA-PK were both present, the Ku and DNA-PK appeared to assume adjacent positions near the terminus. This supports our data from the biochemical studies indicating that both DNA-PK and Ku bind DNA, and yet there is stimulation of DNA-PK by Ku in a manner which is not dependent on collisional interaction. The sliding of Ku along the DNA after loading at an end would allow it to take up a position internal to DNA-PK at the terminus. We are continuing AFM studies to investigate further the configuration of Ku and DNA-PK at the terminus. We expect that especially valuable insights will be obtained by extending the AFM work into imaging under liquids.

### *Concluding remarks*

In conclusion, DNA-PK is able to bind DNA ends directly and becomes activated for kinase activity. Designation of DNA-PK as a catalytic subunit that is without activity in the absence of Ku is inconsistent with this observation. Ku and DNA-PK appear to both be DNA end-binding proteins *in vitro*, but Ku appears to be able, in addition, to slide to internal positions. The independent binding of DNA-PK and Ku to DNA ends begins to reconcile how mutations in them could have somewhat different phenotypes. Mutations of Ku affect both signal and coding joints in V(D)J recombination (Pergola *et al*., 1993; Taccioli *et al*., 1993; Nussenzweig *et al*., 1996; Zhu *et al*., 1996), whereas mutations in DNA-PK affect primarily coding joints (Lieber *et al*., 1988; Malynn *et al*., 1988; Zhu and Roth, 1995). The stimulation of DNA-PK by Ku may account for the aspects in which they both appear to participate (coding joints). Further work will help determine the interplay between these two important components in double-strand break repair.

## Materials and methods

### *Oligonucleotides*

DNA fragments were synthesized: 14-mer, 5′-GGGCCCGGGACGCG-3′ and 5′-CGCGTCCCGGGCCC-3′; 20-mer, 5′-TIdUAGGCTGTGT-CCTCAGAGG-3′; 21-mer, 5′-AIdUTCCTCTGAGGACACAGCCT-3′; and 79-mer, 5′-GATCCTCTGAGGACACAGCCTTGTATTACTGT-GCAAGACACACAATGAGCAAAAGTTACTGTGAGCTCAACTAA-ACC-3′ and 5′-GATCGGTTTAGTTTGAGCTCACAGTAACTTTTGC-TCATTGTGTGTCTTGCACAGTAATACAAGGCTGTGTACTCAC-GAG-3′. The fragments were purified from 20% denaturing polyacrylamide gel, annealed, and labeled at the 5′ ends with T4 polynucleotide kinase in the presence of [$\gamma$-$^{32}$P]ATP (3000–4000 Ci/mmol, Amersham). The labeled fragments were used for photocrosslinking to proteins and band shift DNA-binding assays. Note that the 14-mer has a considerably higher GC content than the 14-mer used for similar studies previously (Falzon *et al*., 1993). Non-radiolabeled annealed DNA fragments were used also in the *in vitro* kinase assays.

### *Cells*

The pre-B-cell line Reh was grown in suspension to $2\times10^6$ cells/ml in RPMI 1640 medium, 10% FBS, 50 μM β-mercaptoethanol, 100 μg/ml penicillin and streptomycin. HeLa S3 cells were grown in suspension to $2\times10^6$ cells/ml in DMEM medium, 10% FBS, 100 μg penicillin and streptomycin.

### *Purification of Ku and DNA-PK*

Both proteins were purified from nuclear extracts prepared either by treatment of nuclei with DNase I (Sigma) at a concentration of 50 μg/ml (Yaneva *et al*., 1985), or extraction with 0.42 M NaCl (Dignam *et al*., 1983). Ion exchange chromatographies on DEAE–cellulose and phosphocellulose P11 were carried out as described previously (Carter *et al*., 1990). DNA-PK and Ku were separated by gel filtration chromatography on a Superose 6 column (Pharmacia) in the presence of 0.4 M KCl as described (Carter *et al*., 1990). This method for purification of DNA-PK and Ku was designated method A, and the nature of the extraction method, DNase I versus high salt, is always designated.

In addition, the DNA-PK and Ku were each purified according to the protocol recently published (Chan *et al*., 1996) and designated method B.

Immunoaffinity and DNA-affinity chromatographies for purification of Ku were performed as previously described (Yaneva *et al*., 1985; Zhang and Yaneva, 1992).

Recombinant Ku was produced in a baculovirus system; the purification of the recombinant Ku involved chromatographies on $Ni^{2+}$ column (Qiagen), DNA–cellulose (Ono *et al*., 1994), and MonoQ (Pharmacia) columns.

### *Immobilization of DNA-PK and Ku on immunobeads*

20 μl of protein G beads (Sigma) were mixed with 200–500 μl of cell culture supernatant from hybridomas secreting anti-DNA-PK monoclonal antibodies: 42-27, 25-4 or only 18-2; anti-Ku monoclonal antibodies: D6D8, D6D9, 2D9 and anti-p70 (Abu-Elheiga and Yaneva, 1992; Wen and Yaneva, 1992); or anti-c-myc monoclonal antibody. The antibodies bound to the beads overnight at 4°C with stirring. The beads with the antibodies were washed three times with 1 ml of 10 mM Tris–HCl, pH 7.5, 0.15 M NaCl, 0.02% Tween-20, and mixed with 50 μl solution containing antigens: either purified DNA-PK (after gel filtration, method A) or mixture of DNA-PK and Ku (before gel filtration) as indicated. The binding was allowed for 1 h at 4°C with gentle tumbling. The beads with the immune complexes were washed three times with 1 ml of kinase buffer containing 0.5 M NaCl/0.1% NP-40 and twice with 1 ml of kinase buffer only. At the end, the beads were split into two portions: 10 μl were assayed for kinase activity, and 10 μl were subjected to crosslinking to a DNA fragment as described below. In control experiments, 10 μl of such beads were assayed for the presence of DNA-PK and Ku by immunoblotting.

### *Photochemical crosslinking of proteins to DNA*

DNA fragments with 5-IdU (IdU phosphoramidite from Glen Research) incorporated at the second position of each 5′ end were annealed to give an 18 bp ds DNA fragment. Typically, 20 μl samples containing proteins and end-labeled DNA fragment at different molar ratios (1:1 to 4:1 protein to DNA) were placed in 1.5 ml microtubes and preincubated for 20 min on ice in kinase buffer (see above). Exposure to a UV light source (Spectroline, $\lambda_{max}$ = 312 nm) was on ice at a distance of 2.5 cm, filtered through a polystyrene Petri dish in a dark room. Crosslinked

products were separated by 8% SDS–PAGE. The gels were dried and either exposed on Kodak film or quantitated on a phosphorimager. In preliminary experiments it was determined that: (i) the maximum crosslinking was after 30 min of irradiation without significant destruction of the proteins; (ii) no crosslinking of DNA to a control protein (BSA) occurred at the concentrations used for crosslinking to DNA-PK and Ku under the same experimental conditions and molar ratios; and (iii) the efficiency of crosslinking was comparable with that reported (Willis *et al*., 1993).

In specified experiments, indicated amounts of excess supercoiled plasmid were added as competitor to challenge the binding of DNA-PK for the linear fragment.

### *Electrophoretic mobility shift assay*

In 20 µl reactions, 0.4 ng (30 fmol) end-labeled DNA fragment was mixed with purified DNA-PK or Ku proteins in the absence or presence of various purified monoclonal antibodies as indicated. The incubation buffer was the same as for the kinase activity assays (see 'Phosphorylation assay'). The reaction mixtures were incubated at room temperature for 15 min, and analyzed by electrophoresis in 5% PAGE as described previously (Zhang and Yaneva, 1992). The reactions containing specific antibodies were incubated for 30 min on ice before addition of the DNA fragment. All monoclonal antibodies used in this assay were purified on protein G–Sepharose (Pharmacia), and stored in PBS. Different highly purified preparations of DNA-PK always resulted in a mobility shift; some preparations show DNA-PK protein aggregation that fails to enter the gel and traps ds DNA oligo in the base of the well. This accounts for the large amount of radiolabel remaining in the well.

### *Phosphorylation assays*

Kinase assays were performed using dephosphorylated casein as substrate as previously described (Carter *et al*., 1990), except that phosphorylated casein was separated and quantitated on a 10% SDS gel. Phosphorylation reactions were in a final volume of 30 µl with a buffer composition as follows: 20 mM Tris–HCl, pH 7.9, 50 mM KCl, 10 mM $MgCl_2$, 1 mM EDTA, 1 mM EGTA, 2 mM DTT, 0.02% Tween-20, 10% glycerol, 200 ng sheared salmon sperm DNA, 20 µg casein, 10 nM [$\gamma$-$^{32}$P]ATP (3000–4000 Ci/mmol, Amersham). Reactions were incubated for 10 min at 37°C and terminated by addition of SDS sample buffer. Phosphorylated casein was separated by 10% SDS–PAGE; the gel was dried and autoradiographed or quantitated using a phosphorimager. The activity was measured by fold increase of radioactivity incorporated into the casein in the presence of DNA compared with the background radioactivity incorporated in the absence of DNA.

Phosphorylation of p53 synthetic peptide was performed as previously described (Finnie *et al*., 1995) except that the DNA-PK was immobilized through the antibodies on protein G beads instead of on DNA cellulose. The beads were incubated with the wild-type or mutant p53 peptide for 10 min at 37°C under the conditions for incubation of DNA–cellulose-immobilized DNA-PK (Finnie *et al*., 1995). Phosphorylated peptide was spotted on phosphocellulose paper, washed with 15% acetic acid, and the incorporated radiolabel was counted (Cherenkov).

### *Immunoblotting*

Western immunoblot analysis was performed as described (Yaneva *et al*., 1985). DNA-PK was detected using 18-2, 25-4 and 42-27 monoclonal antibodies (Carter *et al*., 1990). Ku polypeptides were detected using a mixture of monoclonal antibodies D6D8, RZ2, D6D9 and anti-p70 (Wen and Yaneva, 1990; Abu-Elheiga and Yaneva, 1992). All antibodies were produced in and used as hybridoma cell culture supernatants; all the antibodies were IgG1 type, except 25-4 as noted above. The antigen–antibody complexes were visualized using horseradish peroxidase with an enhanced chemiluminescence (ECL) kit (Amersham).

### *Atomic-force microscopy*

*Sample preparation–optimization and control of immobilization.* AFM samples were prepared by placing a 0.5–2.0 µl drop of solution on freshly cleaved mica which, after ~5 s, was washed-off with 100 µl of sterile, distilled grade-1 water, followed by blow-drying with a stream of dry nitrogen. Experiments with plain buffer solutions showed a typical background in the form of unidentified particulates with sizes $<$50 nm, and these did not exceed 1 particle per 1 µm$^2$. Preliminary experiments with solutions of DNA-PK and Ku revealed in each case the presence of distinct nanoparticulate species of uniform size. The number of these species per unit area exhibited approximately linear dependence on protein concentration, in agreement with their identification as distinct protein molecules. The average number of protein molecules per unit area per 1 nM of protein concentration in solution used for deposition was equal to 6.0 $\pm$ 2.0 molecules/(µm$^2$ nM) for DNA-PK and 1.5 $\pm$ 0.3 molecules/(µm$^2$ nM) for Ku. Subsequent experiments were usually performed with solution concentrations resulting in coverages of ~30 molecules/µm$^2$ and below to avoid excessive overlap of protein–DNA complexes.

The pH 7.9 kinase buffer (see 'Phosphorylation assays') contained 10 mM $Mg^{2+}$, and was expected to be sufficient for DNA binding (Hansma and Laney, 1996). However, in preliminary experiments the success rate for DNA deposition on mica with this buffer was $<$50%. The success rate for DNA deposition was significantly improved when DNA was deposited from a similar buffer, in which Tris was replaced by HEPES. Thus, in subsequent experiments we mixed protein(s) and DNA at higher concentrations in kinase buffer and, after incubation, diluted the solutions to target concentration for deposition in HEPES-based buffer. The number of protein molecules per unit area did not exhibit pronounced dependence on the type of buffer.

We used an 841 bp PCR fragment as the DNA target that was purified from the PCR reaction mixtures using a Qiagen PCR purification kit. The final DNA samples were extracted with phenol/chloroform, precipitated with 70% ethanol and dissolved in TE buffer at a concentration of 0.3 mg/ml.

*AFM imaging.* AFM (Binnig *et al*., 1986) provides a three-dimensional image of a surface. This is accomplished by monitoring the motion of an ultra-sharp-tip micro cantilever scanned in an XY raster above the surface and interacting with it through intermolecular and surface forces. The resolution of this technique is determined by the radius of the probe-tip, which for etched silicon probes used throughout this study is typically of the order of 10–20 nm. In tapping mode AFM (Zhong *et al*., 1993), the cantilever is oscillated above the surface at a frequency close to its resonance frequency (typically ~ 50–300 kHz).

All work described was performed with the aid of Nanoscope III-M system (Digital Instruments, Santa Barbara, CA) operating in tapping mode and equipped with J-type vertical engage piezoelectric scanner. Standard etched silicon probes (l = 120 µm, spring constant ~50 N/m, resonance frequency ~300 kHz) were used throughout the study. Typical scan frequencies were between 1.5 Hz and 5.01 Hz, depending on scan fields which varied from 500 nm×500 nm to 4 µm×4 µm. Through extensive experimentation with tapping-mode imaging of DNA and DNA–protein complexes, we have determined that superior resolution was achieved with minimal cantilever oscillation amplitude (typically $<$10 nm) and with set-point ratios of 0.95 and higher. Additional improvement of resolution is observed when imaging in an atmosphere of helium gas (Hansma *et al*., 1993).

## Acknowledgements

The authors thank Robert B.West and other members of the Lieber laboratory for discussions that were extremely helpful. M.R.L. is supported by the Leukemia Society of America, and this work was supported by funding from the National Institutes of Health to M.R.L. Questions regarding AFM should be referred to T.K. (e-mail: tomek@wuchem.wustl.edu). T.K. wishes to thank Professor J.Schaefer (Washington U.) for support through NIH (GM51554) and Sneha Sastry for technical assistance.

## References

Abu-Elheiga,L. and Yaneva,M. (1992) Antigenic determinants of the 70-kDa subunit of the Ku autoantigen. *Clin. Immunol. Immunopathol.*, **64**, 145–152.

Anderson,C.W. and Carter,T.H. (1996) The DNA-activated protein kinase-DNA-PK. In Jessberger,R. and Lieber,M.R. (eds), *Molecular Analysis of DNA Rearrangements in the Immune System*. Springer-Verlag, Heidelberg, pp. 91–112.

Anderson,C.W. and Lees-Miller,S.P. (1992) The nuclear serine/threonine protein kinase DNA-PK. *Crit. Rev. Euk. Gene Exp.*, **2**, 283–314.

Binnig,G., Quate,C. and Gerber,C. (1986) Atomic force microscope. *Phys. Rev. Lett.*, **56**, 930–933.

Brush,G., Anderson,C.W. and Kelly,T.J. (1994) The DNA-activated protein kinase is required for the phosphorylation of replication protein A during SV40 DNA replication. *Proc. Natl Acad. Sci. USA*, **91**, 12520–12524.

Bustamante,C. and Rivetti,C. (1996) Visualizing protein–nucleic acid interactions on a large scale with the scanning force microscope. *Annu. Rev. Biophys. Biomol. Struct.*, **25**, 395–429.

Cantor,C.R. and Schimmel,P.R. (1980) *Biophysical Chemistry*. W.H.Freeman and Co., San Francisco, CA.

Carter,T.H., Vancurova,I., Sun,I., Lou,W. and DeLeon,S. (1990) A DNA-activated protein kinase from HeLa cell nuclei. *Mol. Cell. Biol.*, **10**, 6460–6471.

Chan,D.W. and Lees-Miller,S.P. (1996) The DNA-dependent protein kinase is inactivated by autophosphorylation of the catalytic subunit. *J. Biol. Chem.*, **271**, 8936–8941.

Chan,D.W., Mody,C.H., Ting,N.S. and Lees-Miller,S.P. (1996) Purification and characterization of the double-stranded DNA-activated protein kinase, DNA-PK, from human placenta. *Biochem. Cell. Biol.*, **74**, 67–73.

deVries,E., Driel,W.v., Bergsma,W.G., Arnberg,A.C. and van der Vliet,P.C. (1989) HeLa nuclear protein recognizing DNA termini and translocating on DNA forming a regular DNA–multimeric protein complex. *J. Mol. Biol.*, **208**, 65–78.

Dignam,J.D., Lebovitz,R. and Roeder,R.G. (1983) Accurate transcription initiation by RNA polymerase II in a soluble extract from isolated mammalian nuclei. *Nucleic Acids Res.*, **11**, 1475–1489.

Dvir,A., Stein,L.Y., Calore,B.L. and Dynan,W.S. (1993) Purification and characterization of a template-associated protein kinase that phosphorylates RNA polymerase II. *J. Biol. Chem.*, **268**, 10440–10447.

Falzon,M., Fewell,J. and Kuff,E.L. (1993) EBP-80, a transcription factor closely resembling the human autoantigen Ku, recognizes single- to double-strand transitions in DNA. *J. Biol. Chem.*, **268**, 10546–10552.

Finnie,N.J., Gottlieb,T., Blunt,T., Jeggo,P. and Jackson,S.P. (1995) DNA-dependent protein kinase activity is absent in xrs-6 cells: implications for site-specific recombination and DNA double-strand break repair. *Proc. Natl Acad. Sci. USA*, **92**, 320–324.

Gottlieb,T. and Jackson,S.P. (1993). The DNA-dependent protein kinase: requirement for DNA ends and association with Ku antigen. *Cell*, **72**, 131–142.

Hansma,H. and Laney,D. (1996) DNA binding to mica correlates with cationic radius: assay by AFM. *Biophys. J.*, **70**, 1933–1940.

Hansma,H. *et al*. (1993) Recent advances in AFM of DNA. *Scanning*, **15**, 296–299.

Jackson,S.P. and Jeggo,P.A. (1995) DNA double-strand break repair and V(D)J recombination: involvement of DNA-PK. *Trends Biochem. Sci.*, **20**, 412–415.

Keller,D. (1991) Reconstruction of STM and AFM images distorted by finite-size tips. *Surf. Sci.*, **253**, 353–364.

Knuth,M.W., Gunderson,S.I., Thompson,N.E., Strasheim,L.A. and Burgess,R.R. (1990) Purification and characterization of proximal sequence element-binding protein 1, a transcription activating protein related to Ku and TREF that binds the proximal sequence element of the human U1 promoter. *J. Biol. Chem.*, **265**, 17911–17920.

Lees-Miller,S.P., Sakaguchi,K., Ullrich,S.J., Appella,E. and Anderson, C.W. (1992) Human DNA-activated protein kinase phosphorylates serines 15 and 37 in the amino-terminal transactivation domain of human p53. *Mol. Cell. Biol.*, **12**, 5041–5049.

Lieber,M.R., Hesse,J.E., Lewis,S., Bosma,G.C., Rosenberg,N., Mizuuchi,K., Bosma,M.J. and Gellert,M. (1988) The defect in murine severe combined immune deficiency: joining of signal sequences but not coding segments in V(D)J recombination. *Cell*, **55**, 7–16.

Lieber,M.R., Grawunder,I., Wu,X. and Yaneva,M. (1997) Tying loose ends: roles of Ku and DNA-dependent protein kinase in the repair of double-strand breaks. *Curr. Opin. Genet. Dev.*, **7**, 99–104.

Malynn,B.A. *et al*. (1988) The *scid* defect affects the final step of the immunoglobulin VDJ recombinase mechanism. *Cell*, **54**, 453–460.

Mimori,T. and Hardin,J.A. (1986) Mechanism of interaction between Ku protein and DNA. *J. Biol. Chem.*, **261**, 10375–10379.

Nussenzweig,A., Chen,C., Sores,V.d.C., Sanchez,M., Sokol,K., Nussenzweig,M.C. and Li,G.C. (1996) Requirement for Ku80 in growth and immunoglobulin V(D)J recombination. *Nature*, **382**, 551–555.

Ono,M., Tucker,P.W. and Capra,J.D. (1994) Production and characterization of recombinant human Ku antigen. *Nucleic Acids Res.*, **22**, 3918–3924.

Pan,Z., Amin,A.A., Gibbs,E., Niu,H. and Hurwitz,J. (1994) Phosphorylation of the p34 subunit of human single-stranded-DNA-binding protein in cyclin A-activated G1 extracts is catalyzed by cdk-cyclin A complex and DNA-dependent protein kinase. *Proc. Natl Acad. Sci. USA*, **91**, 8343–8347.

Pergola,F., Zdzienicka,M.Z. and Lieber,M. (1993) V(D)J recombination in mammalian cell mutants defective in DNA double-strand break repair. *Mol. Cell. Biol.*, **13**, 3464–3471.

Shao,Z., Yang,J. and Somlyo,A. (1995) Biological atomic force microscopy: from microns to nanometers and beyond. *Annu. Rev. Cell. Dev. Biol.*, **11**, 241–265.

Singleton,B., Priestley,A., Steingrimsdottir,H., Gell,D., Blunt,T., Jackson,S., Lehman,A. and Jeggo,P. (1997) Molecular and biochemical characterization of xrs mutants defective in Ku80. *Mol. Cell. Biol.*, **17**, 1264–1273.

Stump,W.T. and Hall,K.B. (1995) Crosslinking of an iodo-uridine-RNA hairpin to a single site on the human U1A N-terminal RNA binding protein. *RNA*, **1**, 55–63.

Suwa,A., Hirakata,M., Takeda,Y., Jesch,S., Mimori,T. and Hardin,J.A. (1994) DNA-dependent protein kinase (Ku protein-p350 complex) assembles on double-stranded DNA. *Proc. Natl Acad. Sci. USA*, **91**, 6904–6908.

Taccioli,G.E., Rathbun,G., Oltz,E., Stamato,T., Jeggo,P.A. and Alt,F.W. (1993) Impairment of V(D)J recombination in double-strand break repair mutants. *Science*, **260**, 207–210.

Wen,J. and Yaneva,M. (1990) Mapping of epitopes on the 86 kDa subunit of the Ku autoantigen. *Mol. Immunol.*, **27**, 973–980.

Wen,J. and Yaneva,M. (1992) Non-linear epitopes of the large subunit of Ku autoantigen recognized by monoclonal and autoantibodies. *Mol. Immunol.*, **29**, 1427–1435.

Williams,P., Shadesheff,K., Davies,M., Jackson,D., Roberts,C. and Tendler,S. (1996) Towards true surface recovery: studying distortions in scanning probe microscopy image data. *Langmuir*, **12**, 3468–3471.

Willis,M.C., Hicke,B., Uhlenbeck,O.C., Cech,T.R. and Koch,T.H. (1993) Photocrosslinking of 5-iodouracil-substituted RNA and DNA to proteins. *Science*, **262**, 1255–1257.

Wu,X. and Lieber,M.R. (1996) Protein–protein and protein–DNA interaction regions within the DNA end binding protein Ku70-Ku86. *Mol. Cell. Biol.*, **16**, 5186–5193.

Yaneva,M., Ochs,R., McRorie,D., Zwieg,S. and Busch,H. (1985) Purification of an 86–70 kDa nuclear DNA-associated protein complex. *Biochim. Biophys. Acta*, **841**, 22–29.

Zhang,W.-W. and Yaneva,M. (1992) On the mechanism of Ku protein binding to DNA. *Biochem. Biophys. Res. Commun.*, **186**, 574–579.

Zhong,Q., Inniss,D., Kjoller,K. and Elings,V. (1993) Fractured polymer/silica fiber surface studied by tapping mode AFM. *Surf. Sci.*, **290**, 1688–1692.

Zhu,C. and Roth,D.B. (1995) Characterization of coding ends in thymocytes of scid mice: implications for the mechanism of V(D)J recombination. *Immunity*, **2**, 101–112.

Zhu,C., Bogue,M.A., Lim,D.S., Hasty,P. and Roth,D.B. (1996) Ku86-deficient mice exhibit severe combined immunodeficiency and defective processing of V(D)J recombination intermediates. *Cell*, **86**, 379–389.

*Received on March 6, 1997; revised on May 7, 1997*